

A Search for ${}^6\text{Li}$ in Stars with Planets

Bacham E. Reddy,¹ David L. Lambert,¹ Chris Laws,²
Guillermo Gonzalez,³ Kevin Covey²

¹*Department of Astronomy, University of Texas, Austin, Texas 78712*

²*Department of Astronomy, University of Washington, Seattle, Washington 98195*

³*Department of Physics and Astronomy, Iowa State University, Ames, Iowa, 50011*

18 December 2018

ABSTRACT

Using very high-resolution ($R \sim 125,000$) and high quality ($S/N \geq 350$) spectra, we have searched for ${}^6\text{Li}$ in stars hosting extra-solar planets. From detailed profile-fitting of the Li I resonance line at 6707.7 Å, we find no significant amount of ${}^6\text{Li}$ relative to the ${}^7\text{Li}$ for any of 8 planet bearing stars (${}^6\text{Li}/{}^7\text{Li} \leq 0.0 - 0.03$) with a strong Li I lines. In particular, we do not confirm the presence of ${}^6\text{Li}$ with ${}^6\text{Li}/{}^7\text{Li} = 0.13$ reported by Israelian et al. (2001) for HD 82943, a star with two known planets. Several of the 8 stars plus HD 219542 A, the planet-less primary of a binary, have been identified in the literature as possible recipients of accreted terrestrial material. For all of the planet-hosting stars and an additional 5 planet-less stars, we find no ${}^6\text{Li}$.

Key words: stars: abundances – stars: Li isotopic ratios – stars: atmospheres – stars: extra-solar planets

1 INTRODUCTION

Observers studying the abundance of lithium in stars continue to uncover novel results. A recent novelty concerning main sequence stars was reported by Israelian et al. (2001) from measurements of the lithium isotopic ratio for HD 82943, a star known to host giant planets, and HD 91889, a star similar to HD 82943 but lacking orbiting planets. For HD 91889, analysis of the 6707 Å Li I resonance line showed a complete absence of ${}^6\text{Li}$ (${}^6\text{Li}/{}^7\text{Li} = -0.002 \pm 0.006$, by number) in agreement with theoretical expectation that ${}^6\text{Li}$ but not ${}^7\text{Li}$ is thoroughly destroyed by protons in the pre-main sequence phase when the star possesses a deep convective envelope. The abundance of lithium, that is ${}^7\text{Li}$, at $\log \epsilon(\text{Li}) = 2.52$ is a typical value for a late F-type main sequence star. In striking contrast, HD 82943, a star with a similar total lithium abundance as HD 91889, showed a surprising amount of ${}^6\text{Li}$: the ratio determined was ${}^6\text{Li}/{}^7\text{Li} = 0.126 \pm 0.014$. This extraordinary amount of ${}^6\text{Li}$ was cited by Israelian et al. as probable ‘evidence for a planet (or planets) having been engulfed by the parent star’. Since lithium ${}^6\text{Li}$ and ${}^7\text{Li}$ – would presumably have been preserved in the unfortunate planets, their ingestion added ${}^6\text{Li}$ (and ${}^7\text{Li}$) to the atmosphere cleansed of ${}^6\text{Li}$ in the pre-main sequence phase.

In this paper, we report measurements of the lithium isotopic abundance ratio for 8 stars (including HD 82943) known to host extra-solar planets, and for several similar stars not known to have extra-solar planets. Our principal result is that ${}^6\text{Li}$ is not detected in HD 82943 or other stars.

The next section describing our observations is followed by a thorough description of our method of analysis. We use HD 82943 as one of the stars with which to illustrate our method. After presenting our results for the ${}^6\text{Li}/{}^7\text{Li}$ ratio, we discuss the implications of the non-detections of ${}^6\text{Li}$, as well as offering a few remarks on the lithium abundance in the atmosphere of stars which host extra-solar planets.

2 OBSERVATIONS

The observed stars listed in Table 1 fall into two categories: stars with extra-solar planets, and similar stars for which there are no reported planets. Chosen stars have a Li I 6707 Å line of a strength enabling a meaningful limit (or detection) to be set on the lithium isotopic ratio. Sharp-lined stars were given priority. The star 16 Cyg B, a host for planets but almost lacking in lithium, was observed in order to check on lines that might blend with the Li I 6707 Å feature. Comparison stars of similar atmospheric parameters were observed including HD 91889 with others chosen from surveys for lithium abundances by Balachandran (1990) and Chen et al. (2000).

All of our observations were obtained with the coude echelle cross-dispersed spectrograph *2dcoude* at the W.J. McDonald Observatory’s 2.7m Harlan J. Smith reflector (Tull et al. 1995). The spectrograph was used in its higher resolution mode. The recorded spectrum provides incomplete coverage of 12 orders. The order containing 6707 Å

arXiv:astro-ph/0205268v1 16 May 2002

Table 1. Atmospheric parameters and observational details of the program stars. The absolute magnitudes, ages, and the masses were estimated using Hipparcos parallaxes and the apparent magnitudes combined with the isochrones and the evolutionary tracks computed by Girardi et al. (2000).

Star	T_{eff} (K)	$\log g$ (cm s^{-2})	ξ_t (km s^{-1})	[Fe/H]	M_v	Age (Gyrs)	M/M_{\odot}	Ref ^a
HD 8574	6200	4.20	1.32	0.12	4.00 ± 0.50^b	2.0 ± 2.0^b	1.15	PS
HD 10697	5605	3.96	0.95	0.16	3.73 ± 0.05	7.1 ± 1.0	1.10	GG
HD 52265	6189	4.40	1.30	0.28	4.06 ± 0.05	1.0 ± 0.5	1.20	GG
HD 75289	6140	4.51	1.47	0.28	4.05 ± 0.04	1.0 ± 0.5	1.20	SIM
HD 82943	6010	4.62	1.08	0.32	4.35 ± 0.05	1.0 ± 0.5	1.00	SIM
HD 89744	6338	4.17	1.55	0.30	2.79 ± 0.06	2.0 ± 0.5	1.40	GG
HD 141937	6150	4.30	1.40	0.31	4.20 ± 0.50^b	0.8 ± 2.0^b	1.22	PS
16 Cyg B	5685	4.26	0.80	0.07	4.55 ± 0.02	9.0 ± 1.0	1.00	LG
HD 209458	6063	4.38	1.02	0.04	4.29 ± 0.10	4.0 ± 1.0	1.10	GG
HD 219542 A ^c	5989	4.37	1.20	0.29	4.50 ± 0.50^b	1.0 ± 2.0^b	1.15	RGG
HD 75332 ^c	6305	4.49	1.05	0.24	3.93 ± 0.05	1.0 ± 1.0	1.25	GG
HD 91889 ^c	6070	4.41	1.52	-0.23	3.75 ± 0.03	7.9 ± 0.5	0.95	IS
HD 142373 ^c	5920	4.27	1.1	-0.39	3.62 ± 0.02	5.0 ± 0.5	0.90	CYQ
HD 154417 ^c	5925	4.30	1.1	-0.04	4.46 ± 0.04	4.0 ± 0.5	1.05	CYQ
HD 187691 ^c	6088	4.07	1.35	0.07	3.66 ± 0.03	4.0 ± 0.5	1.25	KF

^a References providing the adopted atmospheric parameters:- CYQ: Chen et al. (2000); GG: Gonzalez et al. (2001); IS: Israelian et al. (2001); KF: Fuhrmann (1998); LG: Laws & Gonzalez (2001); PS: present study; RGG: Gratton et al. (2001); SIM: Santos et al. (2000).

^b Values of M_v and Age are uncertain as stars lack either measured parallax or accurate visual magnitudes.

^c Stars not known to have planets.

covers 25 Å. The resolving power was $R = \lambda/\Delta\lambda = 125,000$, as determined from the widths (FWHM) of thorium lines in the comparison spectrum. The spectra are over-sampled: there are 4.5 pixels per resolution element.

Several exposures of a star were obtained with an exposure time of 15 to 20 minutes with total integration time of around 1 to 2 hours. A ThAr hollow cathode lamp was observed before and after a sequence of exposures on a star. Each image recorded on a Tektronix 2048 × 2048 CCD was processed in the usual way using IRAF subroutines to obtain a one dimensional spectrum. The wavelength calibration was applied to each individual exposure and was accomplished using a third-order polynomial fit to a large number of Th emission lines; this resulted in a typical rms accuracy of 2 mÅ.

Over the course of a sequence of exposures on a given star, the spectrum drifted on the CCD owing to the change in the Earth’s motion, and to instrumental drifts. By cross-correlation, spectra were shifted so that they matched the first spectrum of a sequence. Continuum normalization of the resultant spectrum was achieved by fitting a sixth-order polynomial to each order. The S/N per pixel in the continuum near 6707 Å is listed in Table 2. As a check on the continuum fitting, we compare the spectrum of HD 82943 near 6707 Å with that of the solar spectrum published by Hinkle et al. (2000) (Figure 1). It is seen that the line-free intervals in HD 82943 correspond very closely to those in the solar spectrum; the rms differences of about 0.2% are consistent with the S/N ratio of our spectrum of HD 82943.

3 ANALYSIS: PRELIMINARIES

In stellar spectra the Li I resonance doublet with a separation of 0.15 Å between the stronger blue and weaker red components is not resolved into two lines; the stellar line is an asymmetric blend with a greater width than other stellar lines of comparable strength. Addition of ⁶Li with its stronger line almost at the wavelength of the weaker ⁷Li line and its weaker line placed at an additional 0.15 Å to the red introduces a wavelength shift of the blend and increases its asymmetry. Therefore, in order to extract the isotopic ratio from a stellar line, it is necessary to establish an accurate wavelength scale, and to quantify the various factors responsible for the line broadening.

A necessary condition for defining the zero point of the wavelength scale is the determination of the stellar radial velocity. But examination of our spectra shows that it is not a sufficient condition because the radial velocity varies with the strength of the measured line. This is due to velocity shifts induced by the convective motions (granulation) in the stellar atmosphere. The conventional list of factors influencing the width of a weak line like the 6707 Å feature includes the projected rotational velocity ($v \sin i$), the macroturbulence, the microturbulence, and the instrumental profile. It is also necessary to consider the blends that contribute to the stellar 6707 Å line.

Reduced spectra were analyzed independently at the University of Texas (UT) and the University of Washington (UW). Results reported here for the full sample are those from the UT analyses, but are confirmed by the UW results. Some differences in the two approaches are noted later.

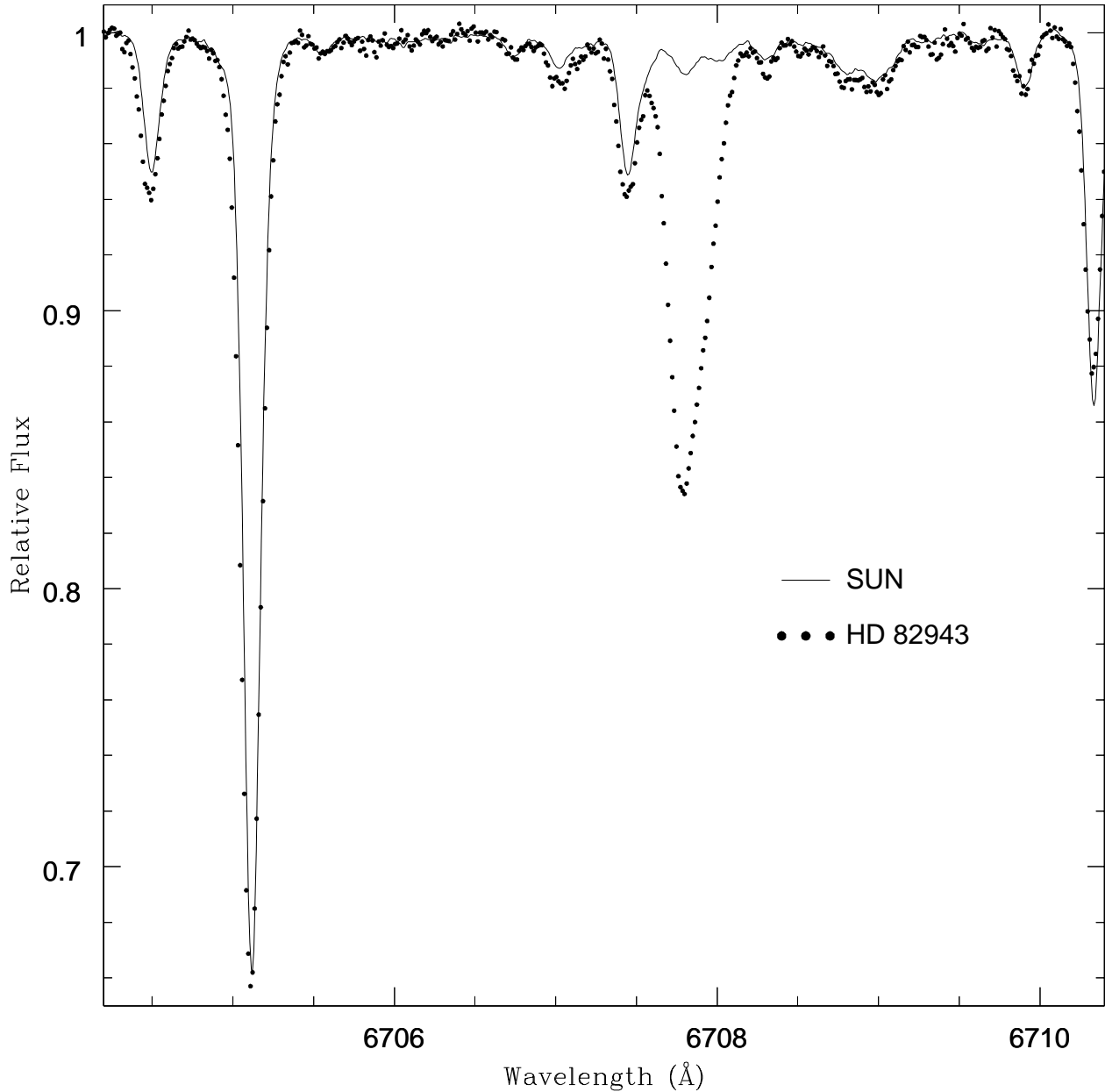


Figure 1. A comparison of the spectrum of HD 82943 and the Sun from 6705 Å to 6710.25 Å. Note the similar strengths and widths of the several Fe I lines but the great difference in the Li I 6707.7 Å feature.

3.1 Radial Velocity and Convective Velocity Shifts

The stellar radial velocity was measured for a sample of unblended Fe I lines using the accurate laboratory wavelengths reported by Nave et al. (1994). There is a clear trend of velocity with equivalent width (W_λ) (Figure 2) in that the weaker lines are blue-shifted with respect to the stronger lines. This is a well known phenomenon attributed to granulation – see the set of extensive measurements on Fe I lines in the Sun and Procyon reported by Allende Prieto & García López (1998) and Allende Prieto et al. (2002), respectively.

The parallel with the Sun is almost exact, as might be expected from Figure 1. Velocities of the same Fe I lines have been measured from Hinkle et al.’s (2000) solar atlas (Figure 2).

Convective shifts are expected to depend on the atom or ion providing the line and on the line’s excitation potential as well as its strength. In order to estimate the shift that might be expected of the Li I resonance line, we measured the solar shifts for lines in the red due to low excitation lines of Na I, Al I, and Ca I: there are few of these lines in the limited bandpass of our stellar spectra. To a satisfactory

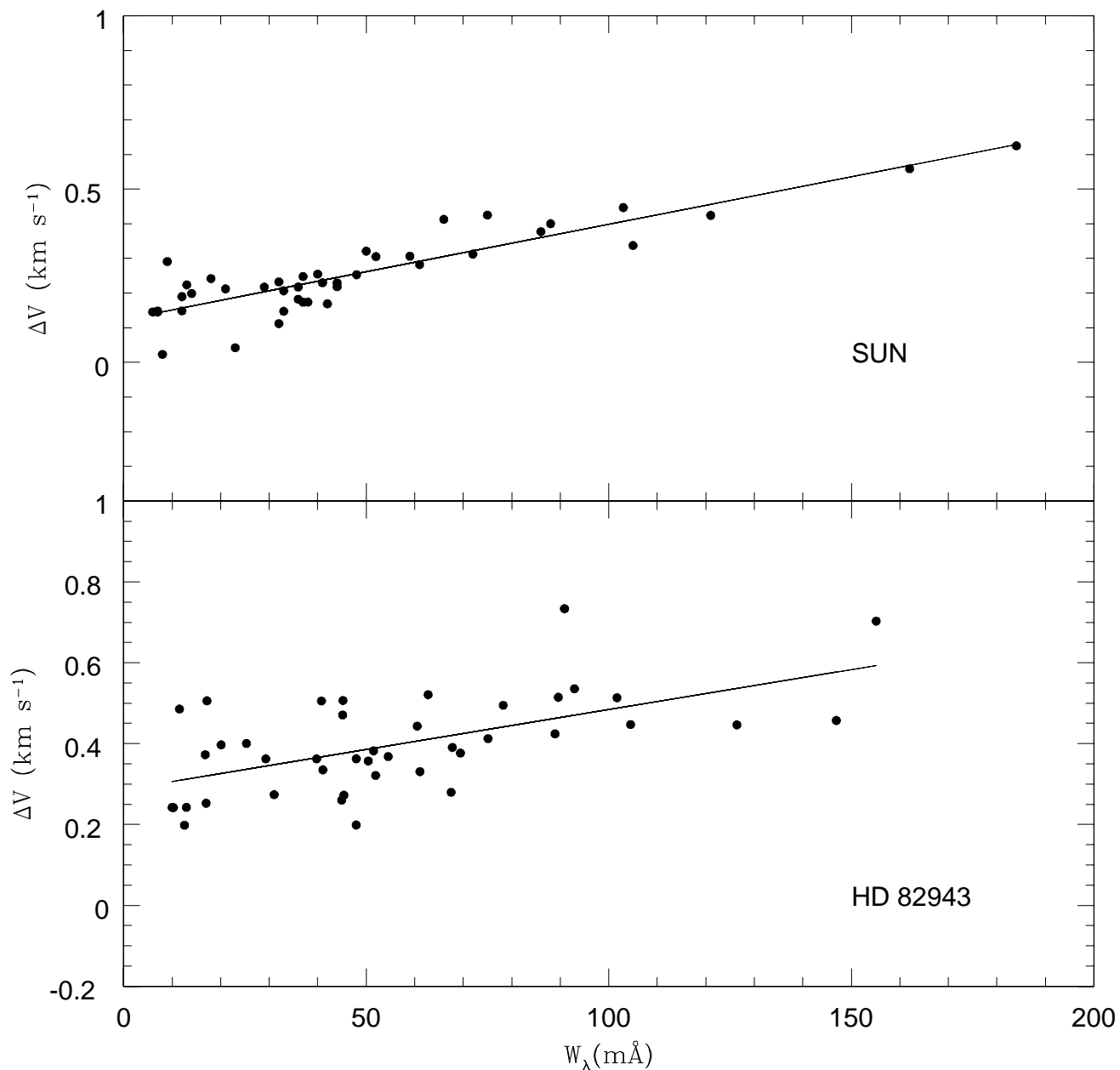


Figure 2. Radial velocity differences for Fe I lines as a function of equivalent width for HD 82943 (bottom panel) and the Sun (top panel). The trend to increasing redshift with increasing equivalent width is similar in the two cases. The solid line is the least squares fit to the data points for HD 82943. The same is shown in the upper panel for the Sun.

precision, the velocity shifts of the additional lines follow the dependence of the Fe I line shifts on W_λ . Since the Fe I shifts for HD 82943 match well the solar shifts, we assume that the same equality holds for the Na I, Al I, and Ca I lines in this star. It should be noted that expected differential velocity shifts between the Li I feature and metal lines in the same order are small ($\sim 0.2 \text{ km s}^{-1}$ or less) relative to the isotopic shift of about 6.7 km s^{-1} but it is, as we note below, an observable effect.

Granulation also renders stellar lines asymmetric. The

line bisector is the usual way to express the asymmetry. Such an asymmetry is measurable for the stellar lines on our spectra. The bisector for a line in our program stars is similar to that of the same line in the solar spectrum. The asymmetry is very much smaller than the isotopic shift of the lithium line.

3.2 Stellar Atmospheric Parameters

Calculation of synthetic spectra requires a model atmosphere, and a line list. A model atmosphere was chosen from the grid provided by Kurucz (1995) according to the parameters T_{eff} , $\log g$, and $[\text{Fe}/\text{H}]$ derived from published abundance analyses (see references given in Table 1. In this analysis we used an updated spectral analysis code MOOG (Snedden, 1973). The lithium isotopic analysis is insensitive to the particular choice of parameters. This and the fact that the published analyses are comprehensive mean that it is not necessary to derive afresh these parameters. For two stars with extra-solar planets, HD 8574 and HD 141937, with atmospheric parameters unavailable in the literature, the parameters T_{eff} , $\log g$, ξ_t , and $[\text{Fe}/\text{H}]$ were derived using 50 well defined Fe I and 4 Fe II lines with the required oscillator strengths (gf -values) for Fe I lines taken from Nave et al. (1994) and from Giridhar & Ferro (1995) for Fe II lines. We estimate uncertainties of about ± 150 K in T_{eff} , ± 0.25 in $\log g$, 0.25 km s^{-1} in ξ_t , and ± 0.10 in $[\text{Fe}/\text{H}]$.

To match synthetic to observed spectra requires information on the various atmospheric effects that broaden the stellar profiles. The UT analysis considered three Fe I lines in the same echelle order as the Li I feature and of a similar strength to it. They are the lines at 6703.5, 6705.1, and 6713.7 Å. Synthetic profiles were computed using the appropriate model atmosphere, the iron abundance, and the microturbulence to match a Fe I line's equivalent width. Two independent schemes were then employed to fit the synthetic line to the observed line profile. In the first scheme, the synthetic profile was broadened by a Gaussian modeled macroturbulence defined by Γ_g , representing the combined effects of stellar rotation, macroturbulence, and the instrumental profile as provided by the thorium lines in the comparison spectrum. In the second scheme, macroturbulence and rotational broadening were treated as different sources of broadening.

In the first scheme, the Γ_g was varied to match the observed profile of a selected Fe I line with the best fit judged by the reduced χ_r^2 where

$$\chi_r^2 = \frac{1}{d} \sum_1^n \frac{(O_i - P_i)^2}{\sigma^2} \quad (1)$$

where O_i and P_i respectively are the observed and predicted relative fluxes at data point i across the line profile, σ is the rms error of the continuum, $d = n - c$ ($= 22$ for Fe I and 35 for Li I, typically) is the number of degrees of freedom in the fit, n is the number of observed data points involved in the fit, and c is the number of parameters to be determined from the computed line profile fit. Here, c is 3 for Fe I lines (i.e., abundance, radial velocity, and the parameter Γ_g), and 4 for the Li I line with the isotopic ${}^6\text{Li}/{}^7\text{Li}$ ratio as the additional parameter. The run of χ^2 with Γ_g is plotted and the minimum value found.

The agreement between the predicted and the observed profiles is quantified with the χ^2 -test. The fit is considered very good when the $\chi_r^2 \simeq 1$ for the best fit (Bevington & Robinson 1992). For HD 82943, Figure 3 shows the three Fe I profiles and the run of χ_r^2 as a function of Γ_g in the first scheme. Two of the lines are fit with a minimum $\chi_r^2 \simeq 1$, and the third with a slightly higher value. The three results are consistent with a mean value $\Gamma_g = 5.03 \pm 0.12 \text{ km}$

s^{-1} . Such a determination ignores the small line asymmetry. Rotational and instrumental broadening are subsumed into Γ_g .

In the second scheme, all stars were also analyzed with $v \sin i$ and V_m as free parameters. The $v \sin i$ and V_m values are determined for a given Fe abundance (determined from equivalent widths) such that the computed profiles best fit (i.e. minimum χ_r^2 values) the observed Fe profiles. Figure 4 shows the results for an Fe I line for HD 82943 along with a similar star HD 75289. The three Fe I lines were fitted in this way. The quality of the fits to the observed profile is quite similar to that obtained just using Γ_g . Results for Γ_g , V_m and $v \sin i$ are given in Table 2 for all the program stars.

In the UW analysis, the Fe I lines at 5852.2, 6330.9, 6703.5, and 6705.1, and 6715.4 Å were employed to determine the line broadening parameters $v \sin i$ and V_m . Instrumental broadening was handled in the same manner as the UT group and the limb darkening coefficients were estimated using the work of Gray (1992). A linelist for 1 Å regions surrounding each line was prepared via comparison of synthetic profiles generated using the MOOG spectral synthesis code (Snedden, 1973) at 0.001 Å resolution with both the Solar Flux Atlas (Kurucz et al. 1984) and spectra of 16 Cyg B. As in similar prior work by Gonzalez (1998) and Takeda (1995), we discovered that in order to achieve good fits to these Fe I features using accurate atmospheric parameters and accepted values for solar rotational and macroturbulent velocities, it was necessary to both reduce the microturbulent velocity, ξ_t , by a factor of 0.4 and allow for a 0.03 - 0.05 dex offset in $[\text{Fe}/\text{H}]$. Applying this correction factor to ξ_t results in a more accurate $v \sin i$. However, adopting a standard value of ξ_t would still result in a good fit to the line profiles. Synthetic profiles were calculated for each line using Kurucz (1995) model atmospheres, selected according to published values of T_{eff} , $\log g$, and $[\text{Fe}/\text{H}]$ (Table 1); accompanying estimates of ξ_t were adjusted in a manner consistent with that performed to fit the solar spectra. In each case, the precise placement of the continuum level was set to minimize the reduced χ_r^2 values of fits to adjacent continuum regions, and the velocity offset Δv was adjusted to minimize the difference between the centroids of the observed and synthesized Fe lines.

The UW analysis is based on 10-20 thousand synthesized profiles for each line at increments of 0.05 km s^{-1} in both $v \sin i$ and V_m and 0.01 dex in $[\text{Fe}/\text{H}]$. Values of χ_r^2 were calculated for each fit, resulting in 2-dimensional grids of χ_r^2 as a function of $v \sin i$ and V_m for 4-7 values of $[\text{Fe}/\text{H}]$. For each Fe I line, we adopt those values of $v \sin i$ and V_m which yielded the minimum values of χ_r^2 amongst all competing fits. We take as our final solution for each star the average of the best-fit broadening parameters found from each line, and quote the standard deviation of their mean as an estimate of uncertainty. The final resulting broadening parameters for the UW group are given in Table 2.

3.3 The Line List around 6707 Å.

Atomic data - wavelengths and gf -values - for the Li I 6707 Å doublet and its isotopic and hyperfine splittings are of very high quality (Smith, Lambert, & Nissen 1998; Hobbs, Thornburn, & Rebull 1999). For the UT line list, potential blending atomic and molecular (CN) lines were identified from

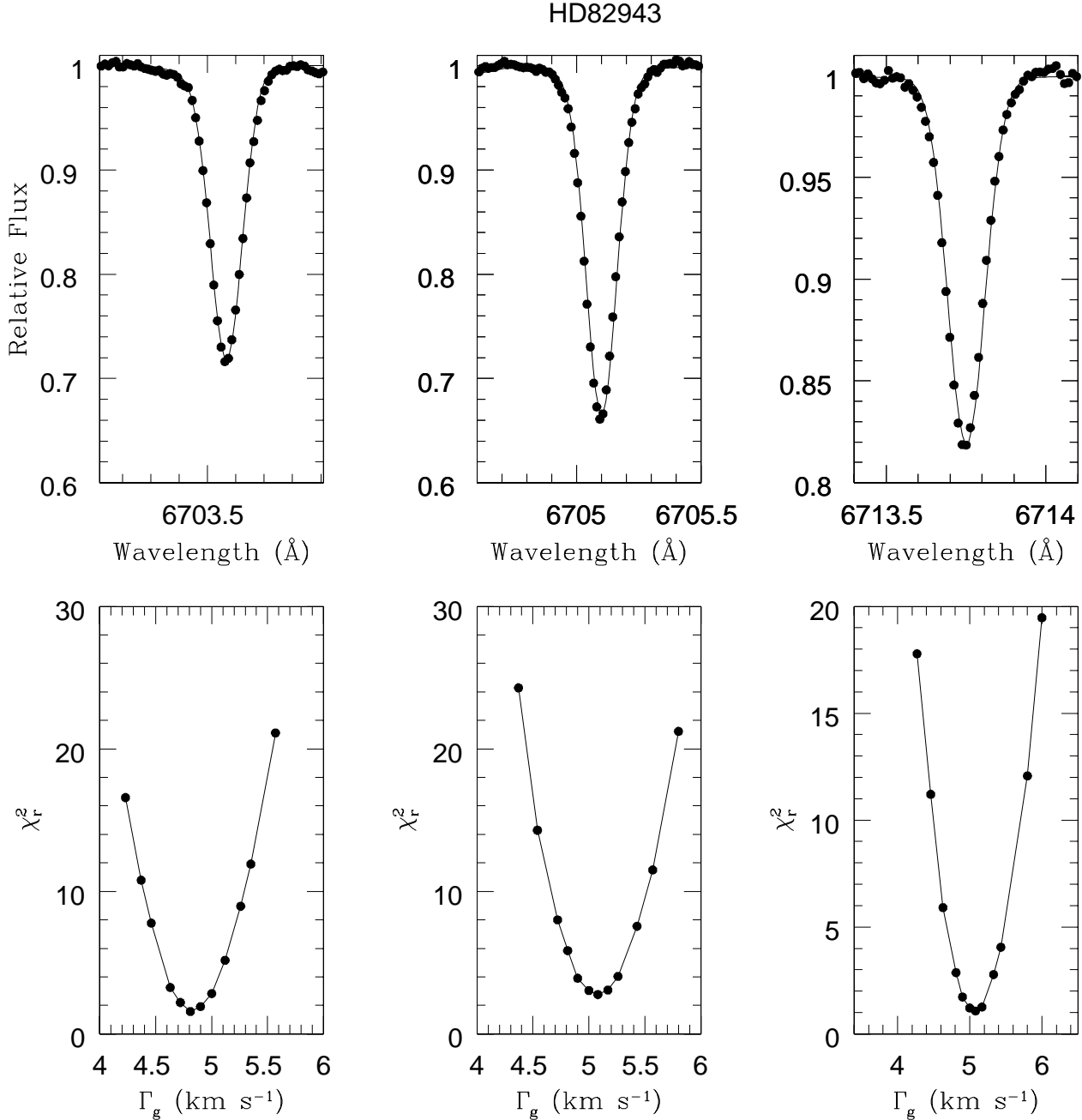


Figure 3. Three Fe I lines in the spectrum of HD 82943 showing the fit of the synthetic profile for the optimum value of the Gaussian macroturbulence Γ_g . The lower panels show the run of χ_r^2 with Γ_g .

various sources: Kurucz (1995), Lambert, Smith, & Heath (1993), Brault & Müller (1975), and Nave et al. (1994). The UT line list was tested and refined by matching the solar spectrum (Hinkle et al. 2000), and the spectrum of 16 Cyg B. Figure 5 shows the fit to the solar and 16 Cyg B spectra suggesting the line list lacks a line at about 6708.0 Å. In their detailed analysis of the solar spectrum around 6707 Å, Brault & Müller noted the presence of weak unidentified lines at 6708.025 Å and 6708.110 Å. Unfortunately, these lines straddle the weaker (red) line of the ${}^6\text{Li}$ doublet, and should, therefore, be included in the line list. On the basis of

laboratory spectra available to them, Brault & Müller concluded that these unidentified lines were not due to either CN or Fe I.

In earlier studies of the 6707 Å line (e.g., Nissen et al. 1999), the presence of the unidentified lines was noted, but ignored as their contribution is negligible for metal-poor dwarfs. However, in F-G main sequence stars of approximately solar metallicity, this pair of lines will significantly affect the red wing of the 6707 Å profile. King et al. (1997) noted the effect of these unidentified lines on the solar ${}^6\text{Li}/{}^7\text{Li}$ ratio. Treating these missing lines as ${}^6\text{Li}$ com-

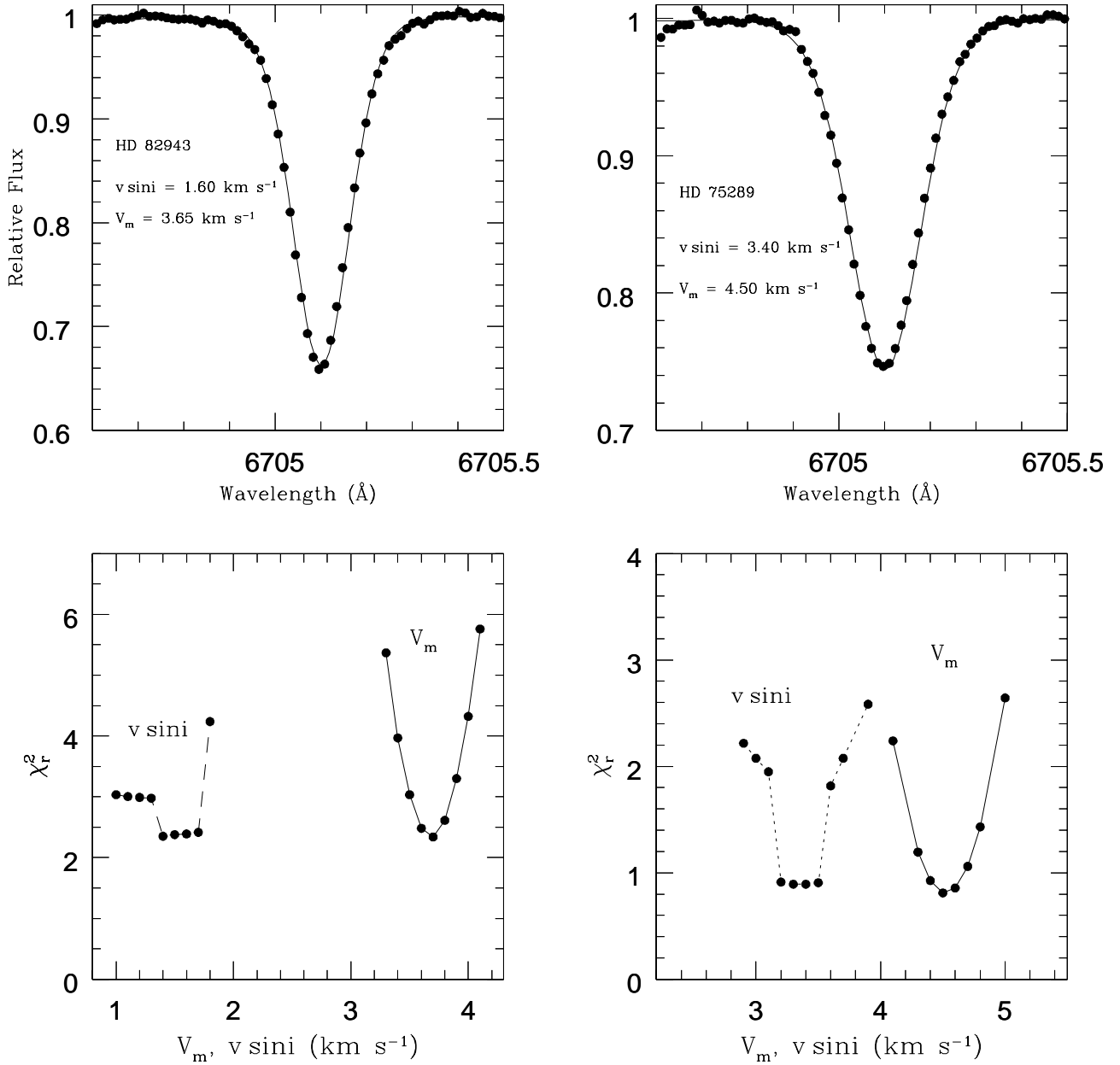


Figure 4. Determination of $v \sin i$ and V_m for HD 82943 and HD 75289

ponents they obtain ${}^6\text{Li}/{}^7\text{Li} = 0.10$ for the Sun. This high Li isotopic ratio for the sun is very unlikely for obvious reasons, and they attributed the lines to Si I. In the solar spectrum, the 6708.025 Å and 6708.110 Å lines have equivalent widths of $W_\lambda = 1.4 \text{ mÅ}$, and $< 0.5 \text{ mÅ}$, respectively. Our analyses of the solar and 16 Cyg B spectra give lithium (${}^7\text{Li}$) abundances consistent with previous analyses. For the Sun, our line list with the Kurucz solar model gives $\log \epsilon(\text{Li}) = 0.98$ and for 16 Cyg B we obtain $\log \epsilon(\text{Li}) = 0.71$ which are close to the values of $\log \epsilon(\text{Li}) = 1.05 \pm 0.06$ and $\log \epsilon(\text{Li}) \leq 0.60$, respectively, derived by King et al. (1997).

Our analysis of selected stars was made first without

the unidentified lines in the line list. Then, we repeated the analysis on the assumption that they were neutral Ti lines with a lower excitation potential of 1.88 eV and derived their gf -values from a fit to the solar spectrum. As a check, we synthesised the spectrum of 16 Cyg B and found that the (unidentified) Ti I lines matched the observed feature well (Figure 5). The star 16 Cyg B is cooler than most of our program stars and is very deficient in lithium (King et al. 1997).

Figure 5 shows that while the ${}^7\text{Li}$ feature gets weaker, the missing feature at 6708.0 Å is a little stronger in 16 Cyg B than in the solar spectrum. We have varied the assumed

Table 2. Lithium isotopic ${}^6\text{Li}/{}^7\text{Li}$ ratio results derived from 6707 Å Li-profile. One- σ errors are quoted.

Star	S/N	Γ_g (km s $^{-1}$)	$v \sin i$ (km s $^{-1}$)	V_m (km s $^{-1}$)	$v \sin i^a$ (km s $^{-1}$)	V_m^a (km s $^{-1}$)	$\log \epsilon(\text{Li})^b$ (dex)	${}^6\text{Li}/{}^7\text{Li}^b$	$\chi_{min}^2{}^b$
HD 8574	300	7.22±0.16	3.30±0.20	4.65±0.10	3.60±0.26	5.30±0.30	2.71±0.05	0.03±0.05	1.02
HD 10697	300	5.27±0.10	1.20±0.30	4.30±0.15	1.61±0.19	4.04±0.18	1.91±0.03	0.00±0.06	1.15
HD 52265	450	7.39±0.08	3.10±0.25	5.50±0.13	3.88±0.11	4.81±0.16	2.76±0.01	0.01±0.03	1.05
HD 75289	350	7.08±0.10	3.40±0.25	4.50±0.10	4.17±0.25	4.15±0.30	2.77±0.02	0.02±0.03	0.90
HD 82943	450	5.03±0.12	1.60±0.20	3.65±0.10	2.09±0.19	3.73±0.13	2.43±0.02	0.00±0.02	1.06
HD 82943 ^c	530	5.00±0.14	1.55±0.13	3.73±0.15	2.43±0.02	0.01±0.03	1.20
HD 89744	550	13.54±0.20	7.60±0.28	8.00±0.20	8.02±0.13	7.71±0.32	2.11±0.01	0.00±0.03	1.20
HD 141937	380	5.14±0.25	1.15±0.30	3.85±0.15	1.89±0.26	4.00±0.29	2.55±0.04	0.01±0.03	1.12
16 Cyg B	600	4.79±0.10	1.60±0.25	3.30±0.18	1.64±0.16	3.49±0.16	0.71±0.02	0.00±0.03	1.30
HD 209458	450	7.24±0.05	3.33±0.15	4.83±0.18	3.57±0.11	5.24±0.22	2.70±0.02	0.00±0.03	0.96
HD 219542 A	300	4.50±0.20	1.55±0.25	3.55±0.10	2.24±0.16	3.66±0.12	2.26±0.03	0.03±0.04	1.06
HD 75332	650	12.62±0.21	8.05±0.20	6.78±0.23	8.20±0.06	6.60±0.16	3.18±0.01	0.00±0.02	1.05
HD 91889	600	6.63±0.12	2.20±0.30	5.15±0.16	2.89±0.26	4.49±0.14	2.46±0.02	0.00±0.02	0.98
HD 142373	700	5.12±0.13	1.05±0.20	4.28±0.15	2.21±0.51	3.67±0.46	2.52±0.01	0.00±0.01	1.36
HD 154417	600	8.68±0.18	3.95±0.32	6.35±0.18	4.90±0.06	5.10±0.12	2.68±0.01	0.00±0.01	1.18
HD 187691	700	6.40±0.08	1.90±0.20	5.25±0.25	2.88±0.12	5.20±0.18	2.56±0.01	0.03±0.02	0.95

^a Values independently derived by UW group.

^b Values computed using the single Gaussian broadening parameter Γ_g .

^c Two spectra of HD 82943 were obtained and independently analysed.

excitation potential of the Ti I lines, and tested to changes in T_{eff} . We found a Ti I line with a LEP of 1.88 eV varies with T_{eff} by around 0.08 dex/100 K, and for a LEP of 0.0 eV, the Ti I line strength varies by 0.12 dex/100 K. Thus, by adopting 1.88 eV lines of neutral Ti for the unidentified lines, instead of 0.0 eV lines, we overestimate their strength by around 0.10 dex for stars of $T_{\text{eff}} = 6400$ K, the hottest stars in our sample. Higher LEP lines of Ti and lines of higher ionisation potential elements like Si and Mg also investigated. Within our T_{eff} range, the T_{eff} effect on strength of these lines does not have noticeable effect on ${}^6\text{Li}/{}^7\text{Li}$ ratios. Given that our programme stars are quite similar to the Sun, identification of the pair as Ti I lines is not critical to the analysis, but their inclusion is critical. The final line list is given in Table 3.

4 THE ${}^6\text{Li}/{}^7\text{Li}$ RATIO

Addition of ${}^6\text{Li}$ to the mix of lithium isotopes shifts the 6707 Å line to the red and increases the line’s asymmetry. For the meteoritic isotopic ratio (${}^6\text{Li}/{}^7\text{Li} \sim 0.10$), the center-of-gravity of the profile shifts redward by ~ 710 m s $^{-1}$ with respect to the ${}^7\text{Li}$ -only profile. Under ideal conditions, where the observed line shifts are independent of their strength and carrier, it is straightforward to determine the wavelength scale from Fe I and other lines and to estimate the ${}^6\text{Li}$ contribution from the 6707 Å line’s wavelength. Convective shifts in the atmosphere introduce a trend in the relation between a line’s wavelength and strength (Figure 2). In the case of HD 82943, the Fe I lines of strength $W_\lambda \approx 50$ mÅ are shifted by 120 m s $^{-1}$ relative to lines of strength $W_\lambda \sim 10$ mÅ. The differential shift is evident from syntheses of the 6707 Å region. When all lines are given an identical radial velocity, it proved impossible to fit simultaneously the Li I line and the adjacent weaker Fe I at 6707.433 Å. While the latter line

was matched in strength and width, the wavelength separation between it and the Li I line was not. When the stellar radial velocity is measured from the Fe I lines at 6703 Å and 6705 Å, a pair of lines similar in strength to the Li line, the observed wavelength of the deepest part of the Li I line is at the predicted wavelength for ${}^6\text{Li}/{}^7\text{Li} = 0.0$ to within about 1 mÅ. This predicted wavelength is moderately sensitive to small amounts of ${}^6\text{Li}$, for example, the shift from ${}^6\text{Li}/{}^7\text{Li} = 0.0$ to 0.1 is 0.005 mÅ (~ 220 m s $^{-1}$), but use of the wavelength is compromised by the presence of convective shifts.

As our primary monitor of the lithium isotopic ratio, we use the profile of the 6707 Å line. This is less affected by the granulation. The Li abundance and the ${}^6\text{Li}/{}^7\text{Li}$ ratios for the program stars are derived with the following procedure by the UT group. Using the model parameters given in Table 2 and the line list given in Table 3, Li-profiles are computed for a given ${}^6\text{Li}/{}^7\text{Li}$ ratio by varying the Li abundance and the wavelength of the Li I line such that the predicted profile fits best the observed profile. We also took the liberty to adjust the observed profile vertically within the rms error ($\sim S/N^{-1}$) of the continuum. Abundances of elements (C, N, Ti, V, and Fe) contributing lines that are blended with the Li-profile are taken from the sources which provided the atmospheric parameters (see Table 1 for references). Predicted profiles are first broadened with the single Gaussian parameter Γ_g and compared with the observed profile. Then, the procedure is repeated but the predicted profiles are broadened using the combination of $v \sin i$, V_m , and the instrumental broadening.

Sample results are shown in Figure 6 for HD 82943 for the case where rotation and macroturbulence are treated as separate effects. Synthetic profiles for the case of Gaussian broadening parameter Γ_g alone are not discernibly different. The agreement between the predicted and the observed profiles is quantified using χ_r^2 . The minimum values, χ_{min}^2 , obtained from χ_r^2 analysis are given in Table 2. In Fig-

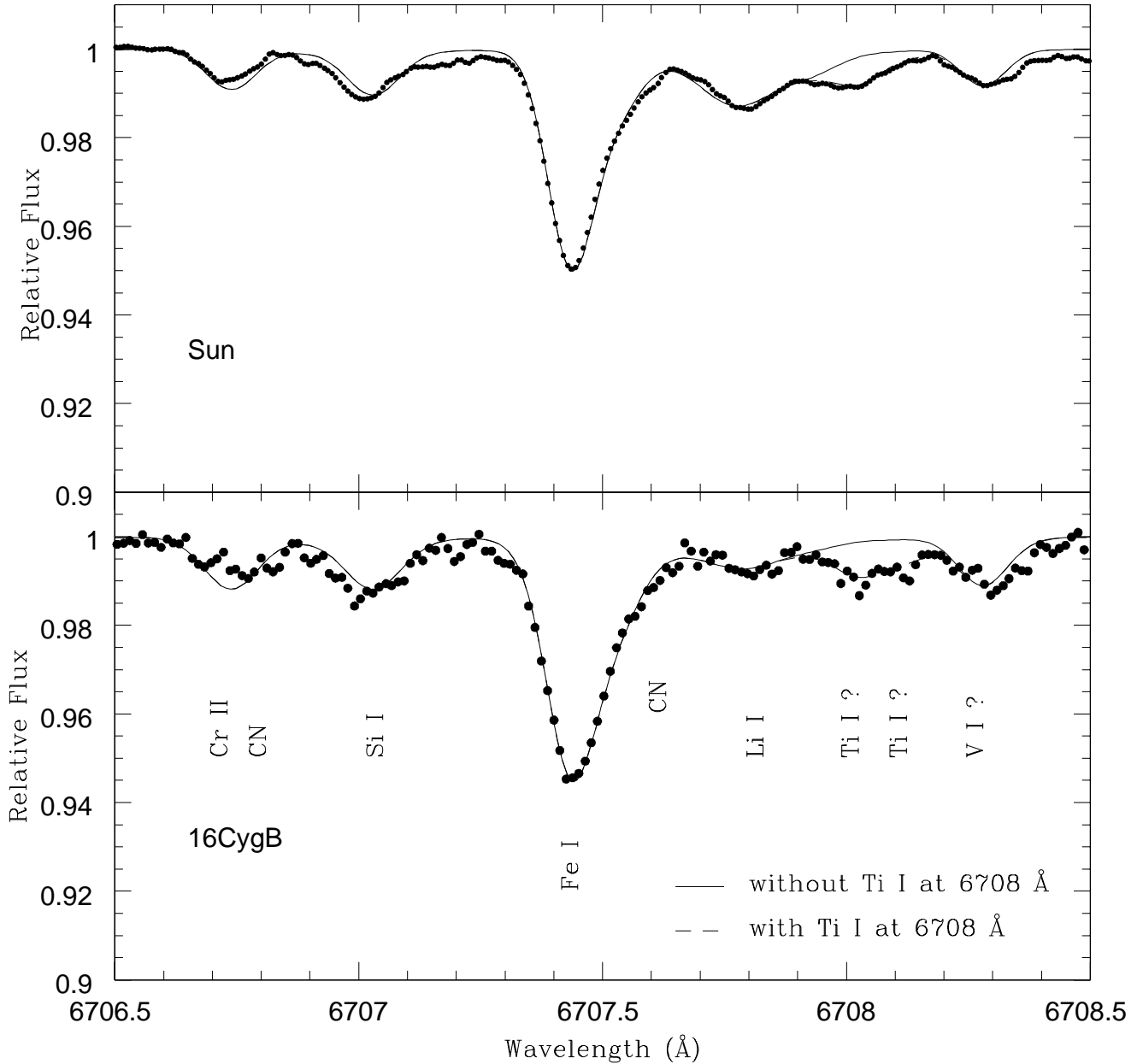


Figure 5. Observed and synthetic spectra around the Li I 6707 Å feature for the Sun and 16 Cyg B. The contribution of the unidentified lines near the weaker ${}^6\text{Li}$ line is given by the difference between the dashed and solid lines between 6707.9 Å and 6708.2 Å.

ure 6, the minimum χ^2 variation values, $\Delta\chi^2$, for HD 82943 obtained for different ${}^6\text{Li}/{}^7\text{Li}$ ratios are plotted. The $\Delta\chi^2$ is computed by subtracting χ_r^2 from the χ_f^2 ; where χ_f^2 is computed by dropping wavelength as a free parameter. The wavelength is fixed for the minimum χ_{min}^2 value from the χ_r^2 analysis. Thus, by definition both the χ_r^2 and χ_f^2 should have the same minimum value of χ_{min}^2 . For HD 82943, we obtained the abundance $\log \epsilon(\text{Li}) = 2.435 \pm 0.005$ and the ratio ${}^6\text{Li}/{}^7\text{Li} = 0.00 \pm 0.03$. The quoted 1- σ errors in the isotopic ratios (Table 3) are obtained from the χ^2 variation, the formal 1- σ , 2- σ , and 3- σ errors (Bevington & Robinson

1992) are indicated in Figure 6. The quoted errors in the $\log \epsilon(\text{Li})$ are 1- σ errors obtained from the χ^2 variation of the Li-profile fitting, and do not include errors arising from the choice of model atmosphere parameters, especially the effective temperature.

In Table 2, we give the results for the lithium abundance and isotopic ratio obtained in the UT analysis using the assumed single line broadening parameter Γ_g . Also, values of χ_{min}^2 for the final best fit between the observed and the predicted Li-profile are given in Table 2. The abundance and the isotopic ratio show very weak dependence on how the

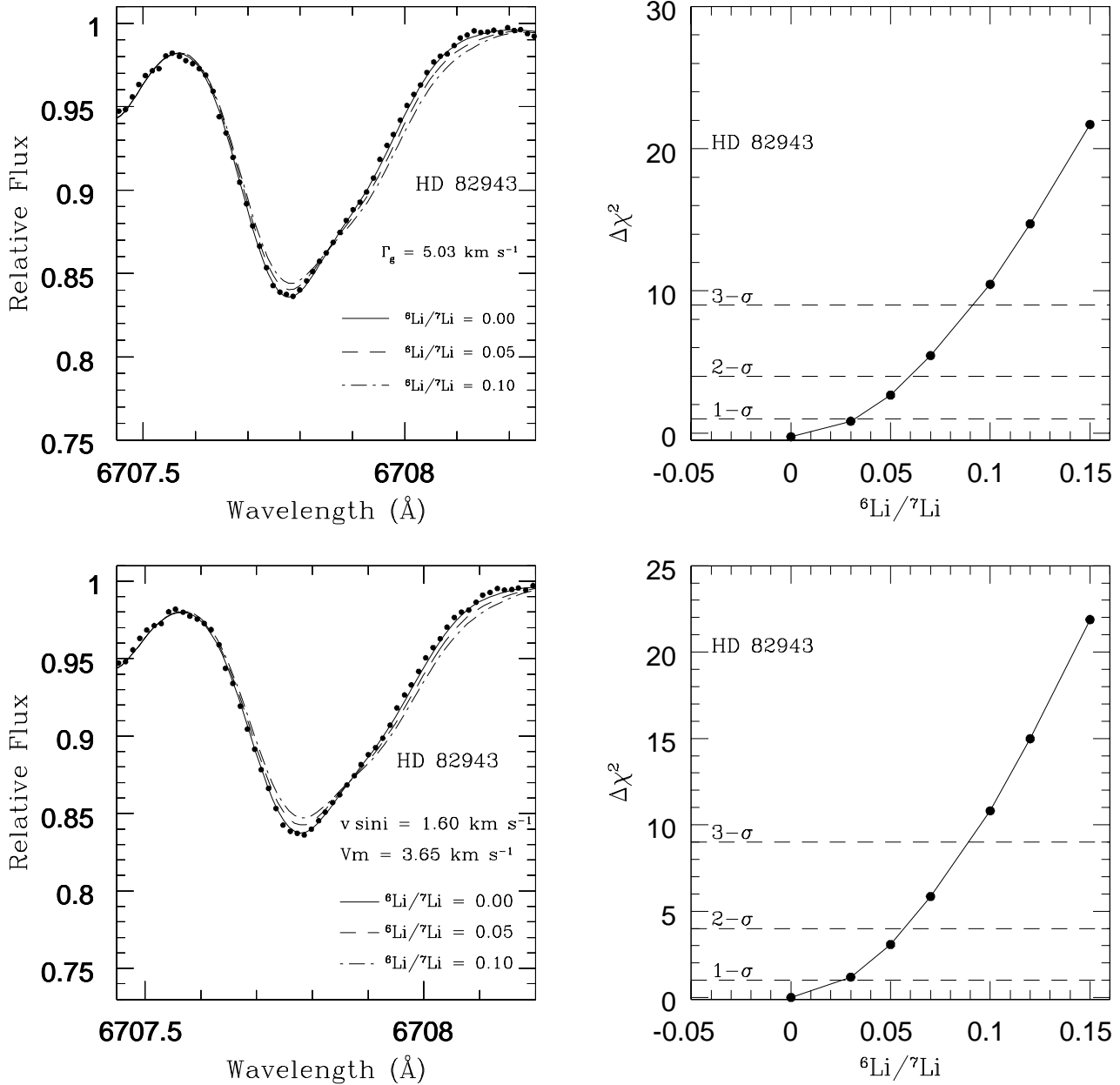


Figure 6. Computed synthetic profiles for different ${}^6\text{Li}/{}^7\text{Li}$ ratios are compared with the observed Li-profile. Computed profiles are broadened with the broadening parameter Γ_g (top panel) and with the separated radial-tangential macroturbulence, rotational velocity and the instrumental profile (bottom panel). The χ^2 variance $\Delta\chi^2$ versus the Li isotopic ratio is shown for both the cases. The errors 1- σ , 2- σ , and 3- σ are noted.

velocity broadening is assigned. Additional examples of observed and synthetic spectra and accompanying plots of χ^2 are shown in Figures 7 & 8. Although the lithium abundance is sensitive to the adopted model atmosphere – temperature is the controlling influence – the isotopic ratio is quite insensitive to it. We repeated the analysis using models drawn from the MARCS grid (Gustafsson et al. 1975) and found no noticeable difference in either the broadening parameters or the Li-isotopic ratio. Table 2 shows that, across the

sample of stars, the lithium is pure ${}^7\text{Li}$ with no convincing detection of ${}^6\text{Li}$. This result holds for stars with and without extra-solar planets.

Our analysis of the 6707 Å line profile using standard model atmospheres obviously neglects the influence of the stellar granulation, which is responsible for the line shifts and asymmetries. These can have only a slight effect on the results. Stellar equivalents of sunspots and faculae might cause the lithium line to be strengthened over a few localized

Table 3. Adopted linelist at the vicinity of the Li 6707Å profile

λ (Å)	Element	LEP (eV)	log gf (dex)
6707.381	CN	1.83	-2.170
6707.433	Fe I	4.61	-2.283
6707.450	Sm II	0.93	-1.040
6707.464	CN	0.79	-3.012
6707.521	CN	2.17	-1.428
6707.529	CN	0.96	-1.609
6707.529	CN	2.01	-1.785
6707.529	CN	2.02	-1.785
6707.563	V I	2.74	-1.530
6707.644	Cr I	4.21	-2.140
6707.740	Ce II	0.50	-3.810
6707.752	Ti I	4.05	-2.654
6707.7561	⁷ Li	0.00	-0.428
6707.7682	⁷ Li	0.00	-0.206
6707.771	Ca I	5.80	-4.015
6707.816	CN	1.21	-2.317
6707.9066	⁷ Li	0.00	-1.509
6707.9080	⁷ Li	0.00	-0.807
6707.9187	⁷ Li	0.00	-0.807
6707.9196	⁶ Li	0.00	-0.479
6707.9200	⁷ Li	0.00	-0.807
6707.9230	⁶ Li	0.00	-0.178
6708.025	Ti I	1.88	-2.252
6708.0728	⁶ Li	0.00	-0.303
6708.094	V I	1.22	-3.113
6708.125	Ti I	1.88	-2.886
6708.280	V I	1.22	-2.178
6708.375	CN	2.10	-2.252

regions of a stellar disk. Consider, for example, a strengthening of the line in an area close to the receding limb of the star. The result would be a red asymmetry to the lithium line, and quite possibly a weaker asymmetry would be imposed on the Fe I comparison lines used to set the broadening parameters. In these circumstances, one might overestimate the contribution of ⁶Li. Similarly, if areas on the approaching limb carry undue weight in forming the profile, the ⁶Li contribution could be underestimated. If a major portion of the Li I line is formed in a few special areas, our theoretical profiles would fail to fit the observed profiles.

Our demonstration that excellent fits to the 6707 Å profiles are possible is a good indication that stellar spots and faculae cannot play an important role. Israelian et al. recognized that a false ⁶Li signal could arise from the neglect of the effects of localized regions on the formation of the 6707 Å line. They advanced cogent reasons - photometric and radial velocity stability - for rejecting this possibility in the case of HD 82943. The fact that our observed profiles are very similar to their profile (see below) is additional evidence that the lithium line is not formed preferentially in a few areas.

4.1 The Case of HD 82943

Israelian et al. (2001) derived the high value of ⁶Li/⁷Li = 0.126 ± 0.014 for HD 82943. Our analysis (UT and UW) shows no indication of ⁶Li or ⁶Li/⁷Li = 0.0 ± 0.03. One can think of two possibilities for the discrepant results: a) a dif-

ference in the observed spectra, and b) differences in the analyses.

Israelian et al.'s spectrum is of similar quality to ours with respect to resolving power (R = 110,000 vs our 125,000) and S/N ratio in the continuum near the Li I line (S/N ~ 500 in both the studies). Comparison of their electronically published Li I profile for HD 82943 with our profiles shows near perfect agreement; the differences are much smaller than those between synthetic profiles for ⁶Li/⁷Li = 0.0 and 0.13.

Given that there is no difference between Israelian et al.'s and our spectra of a size sufficient to account for the different ⁶Li/⁷Li ratios, the sources of the discrepancy must lie in the methods of analysis. In seeking an explanation, we consider the adopted model atmospheres, the fitted line broadening parameters, and the chosen line lists. We adopt the model atmosphere parameters - T_{eff} , log g , [Fe/H], and ξ_t - used by Israelian et al. They do not explicitly indicate the source of the model atmosphere but it is most improbable that given the similarities between modern grids of model atmospheres (see our test of a MARCS model) that an alternative choice can lead to anything but a very small change in the recovered ⁶Li/⁷Li ratio.

In obtaining the broadening parameters, Israelian et al. used two of our three Fe I lines to obtain $v \sin i = 1.65 \pm 0.05 \text{ km s}^{-1}$ and $V_m = 3.90 \pm 0.2 \text{ km s}^{-1}$. These compare well with our values $v \sin i = 1.60 \pm 0.20 \text{ km s}^{-1}$, and $V_m = 3.65 \pm 0.10 \text{ km s}^{-1}$, where we assumed the same form for V_m as Israelian et al. Analysis of our spectrum using their broadening parameters also gives ⁶Li/⁷Li = 0.01, not 0.126. Our result is insensitive to the form adopted (Gaussian macroturbulence vs rotation and macroturbulence) for the line broadening (Figure 9).

The inferred contribution from ⁶Li to the observed profile depends on the completeness and accuracy of the line list. It would appear from their paper that Israelian et al. did not include the unidentified line at 6708.025 Å in their line list, and overlooked the weaker line at 6708.125 Å. The unidentified lines which we assign to Ti I play a role because they lie on either side of the weaker ⁶Li I line. Their combined strength in the solar spectrum is about 1.5 mÅ. In a metal-rich star like HD 82943, their strength is greater than in the Sun. Given that the equivalent width of the 6707 Å feature is 50 mÅ for HD 82943, the lines' estimated contribution of 2.2 mÅ to the weaker ⁶Li line corresponds to ⁶Li/⁷Li ~ 0.06. The linelist compiled independently at the University of Washington differs very little from that in Table 3. Use of this linelist instead of that in Table 3 does not give significantly different synthetic spectra computed for the same input data. Israelian et al. used HD 91889 as a comparison star, but this is not necessarily a perfect foil for eliminating the effects of weak blends. This star is metal-poor with [Fe/H] = -0.23 or 0.55 dex down from HD 82943. This relative metal deficiency plus slight differences in effective temperature and surface gravity mean that unidentified lines like the supposed Ti I lines will be appreciably weaker in HD 91889 than in HD 82943. In contrast, our sample of comparison stars includes examples of similar metallicity to HD 82943.

To investigate further the influence of the unidentified lines, we analysed the HD 82943 profile with different Ti abundances assigned to the pair of unidentified lines. As the abundance is decreased, the drop in absorption from the Ti I

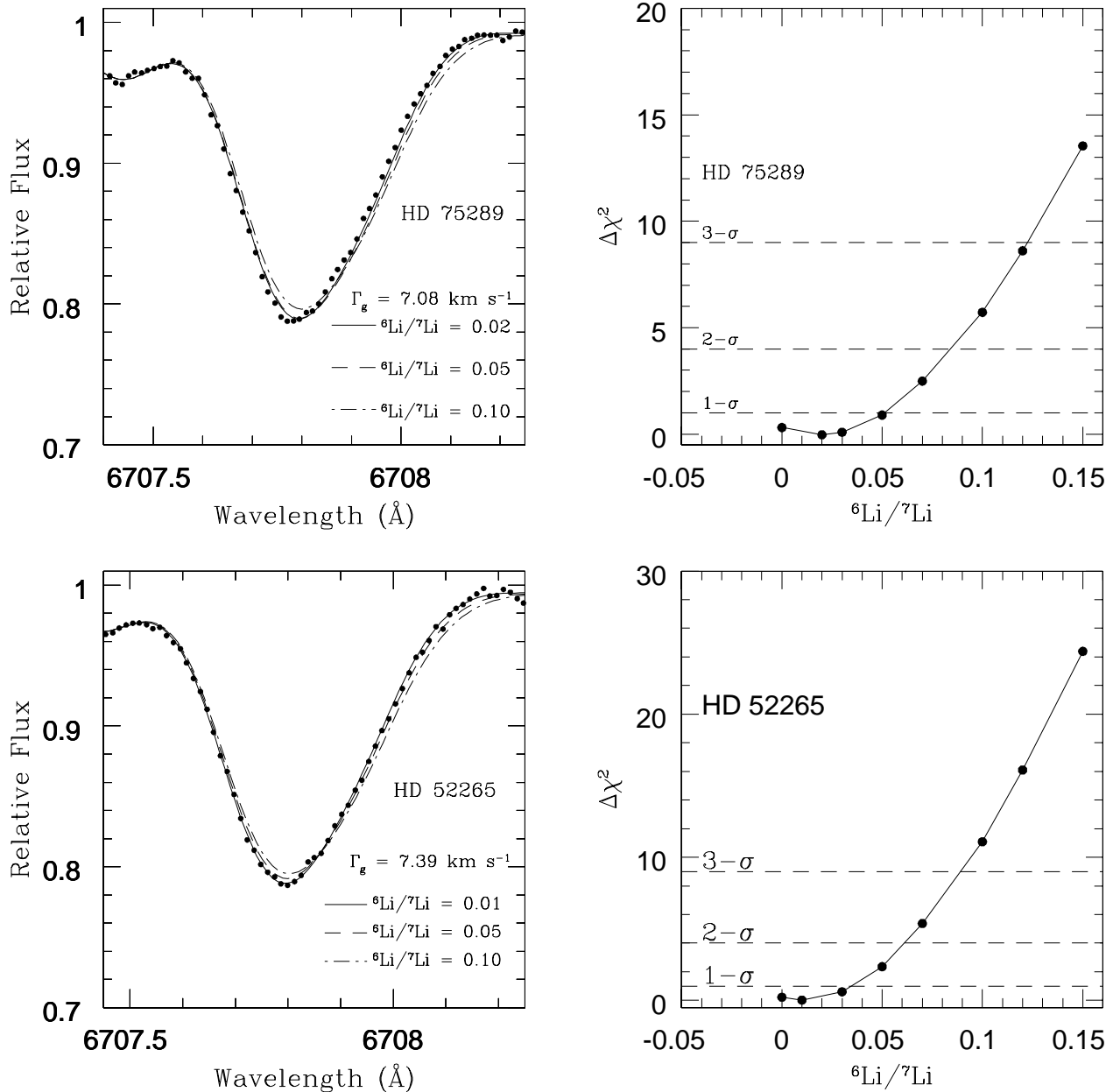


Figure 7. Determination of ${}^6\text{Li}/{}^7\text{Li}$ ratio by fitting the Li-profile for two stars with extra-solar planets: HD 75289 (top panel) and HD 52265 (bottom panel). The χ^2 -test results are shown for both the stars.

lines is compensated for an increasing ${}^6\text{Li}$ abundance, but the quality of the fit to the observed line decreases steadily. This is well shown by Figure 10 where we plot the Ti abundance versus the derived ${}^6\text{Li}/{}^7\text{Li}$ that best fits the line. The exercise was done for Ti I lines of 0.0 eV and 1.88 eV. In the latter case, the χ^2 for the best fit is marked and clearly increases as the contribution of the unidentified lines is reduced.

Our stellar sample include several other metal-rich stars, including one not known to host planets. A plausible assumption is that, if ${}^6\text{Li}$ is present in these stellar atmo-

spheres, the ${}^6\text{Li}/{}^7\text{Li}$ ratio will vary from star-to-star, and is likely absent in the star without planets (HD 75332). Incorrect representation of the list of blending lines could bias the ${}^6\text{Li}/{}^7\text{Li}$ determinations but is unlikely across this sample of metal-rich stars to alter the spread in ${}^6\text{Li}/{}^7\text{Li}$ ratios. The fact that we find ${}^6\text{Li}/{}^7\text{Li} \simeq 0.00$ in all cases suggests that ${}^6\text{Li}$ is not present in these metal-rich stars, including HD 82943. Blends have a smaller effect on the more metal-poor stars. The best fits to the observed profiles are found for ${}^6\text{Li}/{}^7\text{Li} = 0.00$ (i.e., non-negative) is a good indication that the blending lines have not been overestimated.

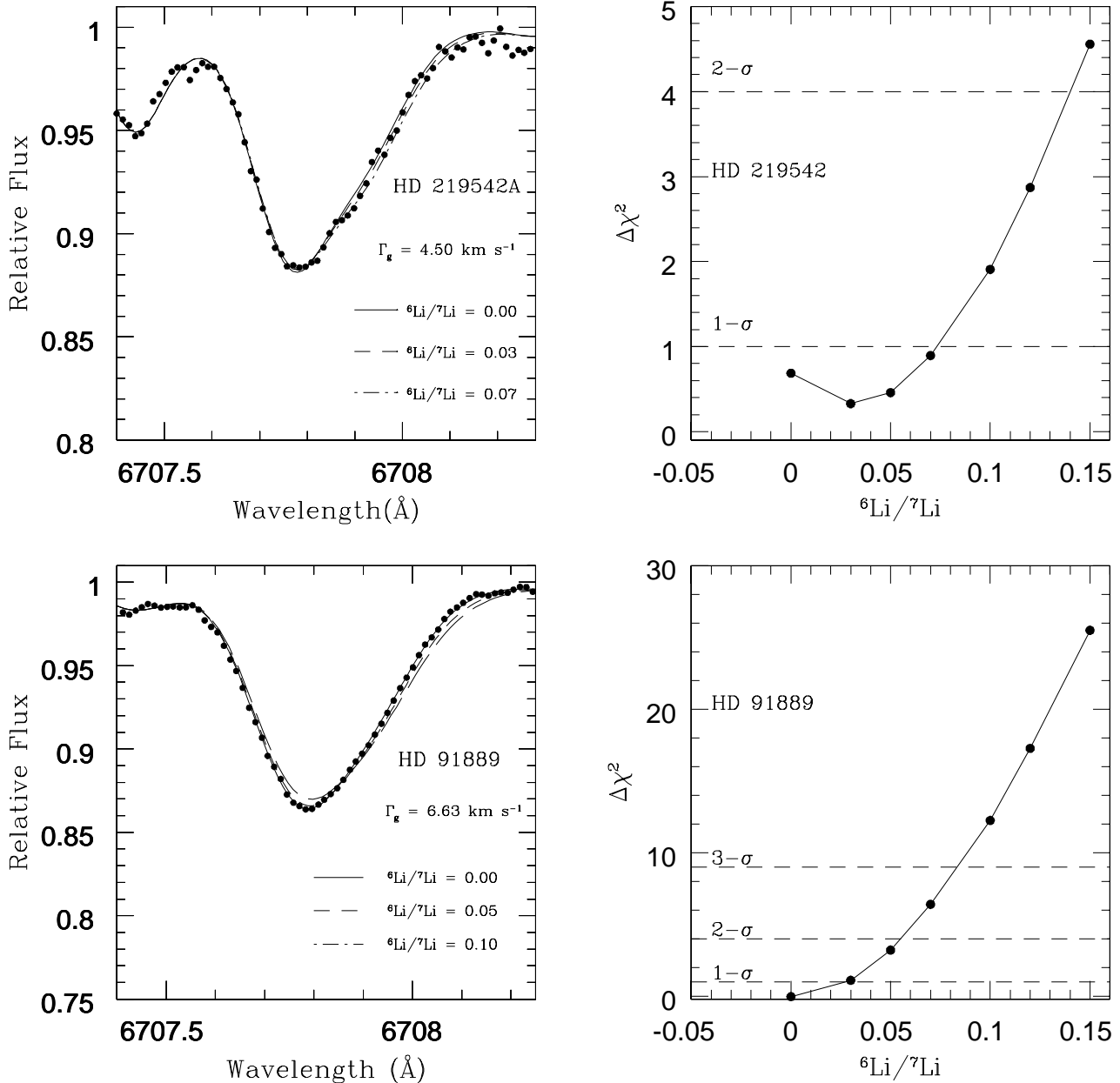


Figure 8. Same as Figure 7. Li-profile fitting and the χ^2 -test results for HD 219542 A (top panel) and HD 91889 (bottom panel) which are not known to have planets. The Li-profile of HD 219542 best fits the computed Li-profile of ${}^6\text{Li}/{}^7\text{Li} = 0.03 \pm 0.04$.

5 DISCUSSION

Our sample of planet-hosting stars are placed in an HR-diagram (Figure 11) as a guide to their evolutionary state. We use the *Hipparcos* parallaxes, the observed V magnitudes (interstellar reddening is neglected), and the reported T_{eff} . On this diagram, we place isochrones from Girardi et al. (2000) for $[\text{Fe}/\text{H}] = 0.0$ and 0.3 and ages from 1 to 9 Gyr. All but three of the stars are young; their ages are 4 Gyr or less (Table 1).

The young stars have a lithium (${}^7\text{Li}$) abundance that

appears normal for stars of their age and metallicity. An empirical demonstration of normality is provided in Figure 12 where the lithium abundance is plotted versus T_{eff} and compared with observations from three open clusters of differing ages – Pleiades at 0.1 Gyr, Hyades at 0.7 Gyr, and M67 at 4.5 Gyr – summarised by Jones, Fischer, & Soderblom (1999). Ages inferred from Figure 11 are consistent with those listed in Table 1. Lithium abundances for our main sequence stars and the clusters are approximately consistent with theoretical predictions (see, for example, Proffitt & Michaud 1989). We note that our sample stars were selected to have mod-

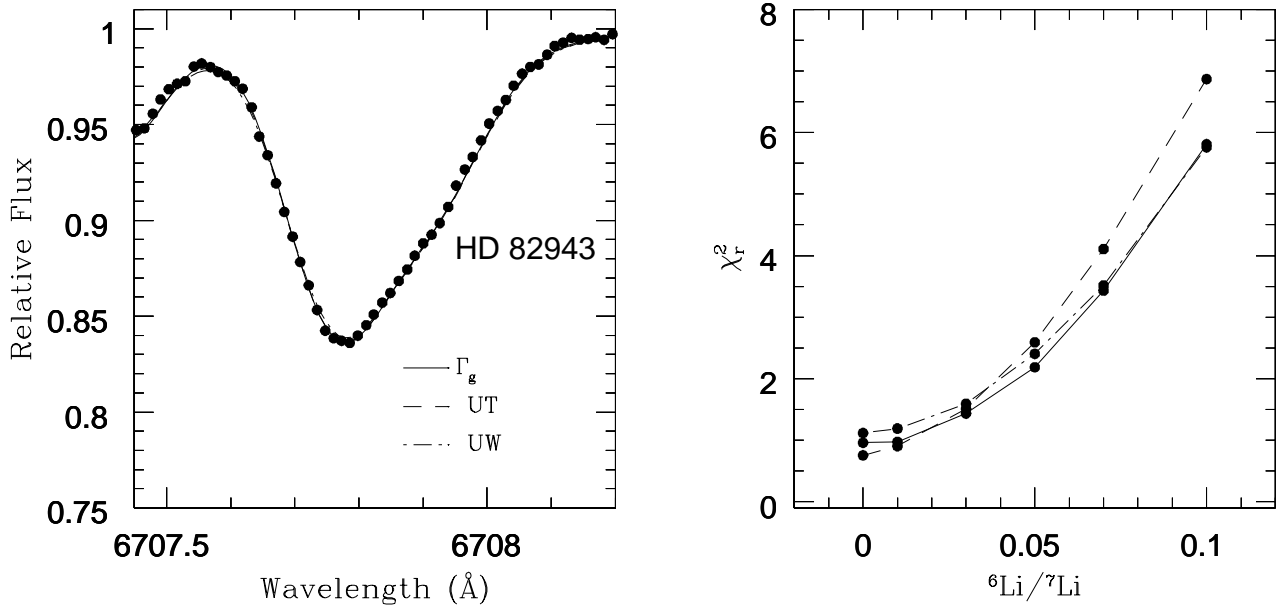


Figure 9. Li-profile fitting for HD 82943 using three different forms of line broadening parameters (left panel): $\Gamma_g = 5.03 \text{ km s}^{-1}$, $v \sin i = 1.60 \text{ km s}^{-1}$, $V_m = 3.65 \text{ km s}^{-1}$ from the UT analysis and $v \sin i = 2.09 \text{ km s}^{-1}$, $V_m = 3.73 \text{ km s}^{-1}$ from the UW analysis. In the right panel we showed χ_r^2 -test analysis for each case. Note a very slight change in the quality of the fit but in all the three cases χ_{\min}^2 is found for ${}^6\text{Li}/{}^7\text{Li} \leq 0.01$.

erate to strong Li lines. So, the plot is necessarily biased towards higher Li abundances.

Normal behaviour for ${}^6\text{Li}$ must be defined on theoretical grounds because there are no observations of this isotope in young stars. Standard models (Proffitt & Michaud 1989) predict effectively complete destruction of ${}^6\text{Li}$ in the pre-main sequence phase. Destruction results when the convective envelope exposes lithium to warm protons at its base. Little to no destruction of ${}^7\text{Li}$ occurs; the (p, α) reactions

occur about 80 times more slowly for ${}^7\text{Li}$ than for ${}^6\text{Li}$. Destruction of ${}^7\text{Li}$ occurs on the main sequence, as revealed by the lowering of the lithium abundance in the older clusters. Loss of lithium is more severe the lower the mass of the star. Since the lithium depletion is driven by exposure to protons, even minor reductions of the ${}^7\text{Li}$ abundance below the value in zero age main sequence stars must be accompanied by very much larger reductions for ${}^6\text{Li}$.

Into this picture for lithium abundances of normal stars

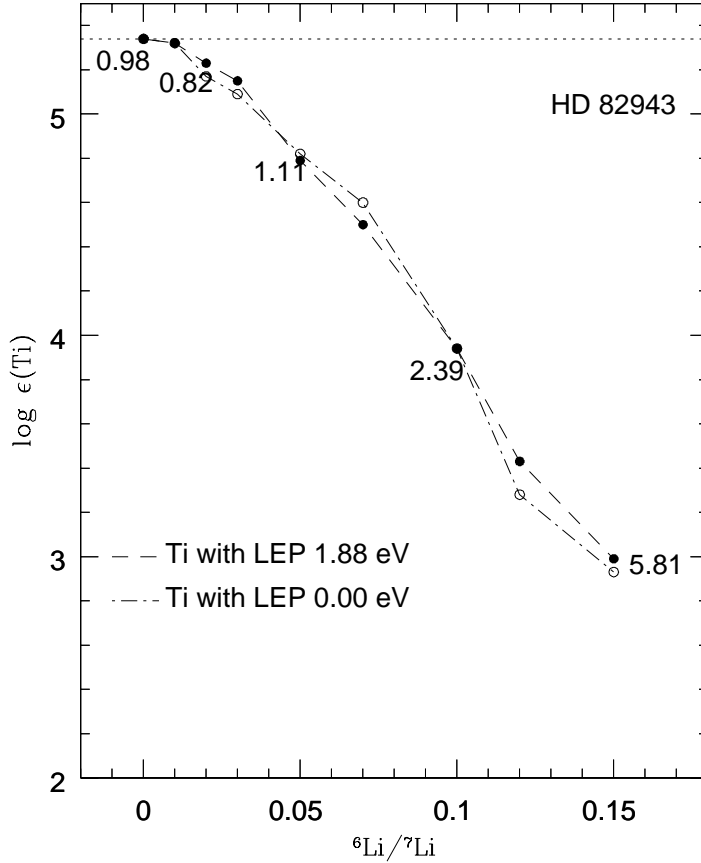


Figure 10. Investigation of the effect of adopted Ti I abundance on the ${}^6\text{Li}/{}^7\text{Li}$ ratio for HD 82943. The dotted horizontal line is the observed Ti I abundance for HD 82943. The numbers are χ^2 -values for the best fits for 1.88 eV case.

must be woven the suggestion that main sequence stars may accrete one or more planets (or circumstellar material) which provide fresh lithium to the star’s convective envelope with the largest effect being a replenishment of the ${}^6\text{Li}$ abundance. After accretion, the ${}^6\text{Li}/{}^7\text{Li}$ ratio in the star’s atmosphere depends primarily on (i) the mass and composition of ingested material relative to the mass and composition of the stellar convective envelope, and (ii) the time elapsed since ingestion. Montalbán & Rebolo (2002) have provided a useful exploration of these dependencies. Their calculations for main sequence stars consider the accretion of 1 to 10 M_J by main sequence stars of masses from about 0.7 M_\odot to 1.2 M_\odot and of two compositions ($[\text{Fe}/\text{H}] = 0.0$ and 0.3). A ratio ${}^6\text{Li}/{}^7\text{Li} \simeq 0.10$ immediately following accretion is achieved, for example, when a giant planet of mass 10 M_J is accreted by a 1.2 M_\odot main sequence. The post-accretion isotopic ra-

tio decreases with decreasing mass of the star because the mass of a main sequence star’s convective envelope increases to lower masses. Accretion increases also the ${}^7\text{Li}$ abundance, that is the ‘total’ lithium abundance. If lithium has not been depleted prior to accretion, the abundance increase is small (about 0.2 dex for accretion levels providing ${}^6\text{Li}/{}^7\text{Li} \sim 0.10$), and, therefore, the total lithium abundance is not a sensitive indicator of the occurrence of accretion.*

Survival of ${}^6\text{Li}$ also determines its detectability. Within the constraints set by plausible assumptions about the ac-

* Similarly, the beryllium abundance is a poor sensor of accretion. In fact, beryllium is largely undepleted in main sequence stars, even in stars showing lithium to be severely depleted. Santos et al. (2002) measured Be abundances to find ‘no clear difference’ between the abundances in stars with and without planets.

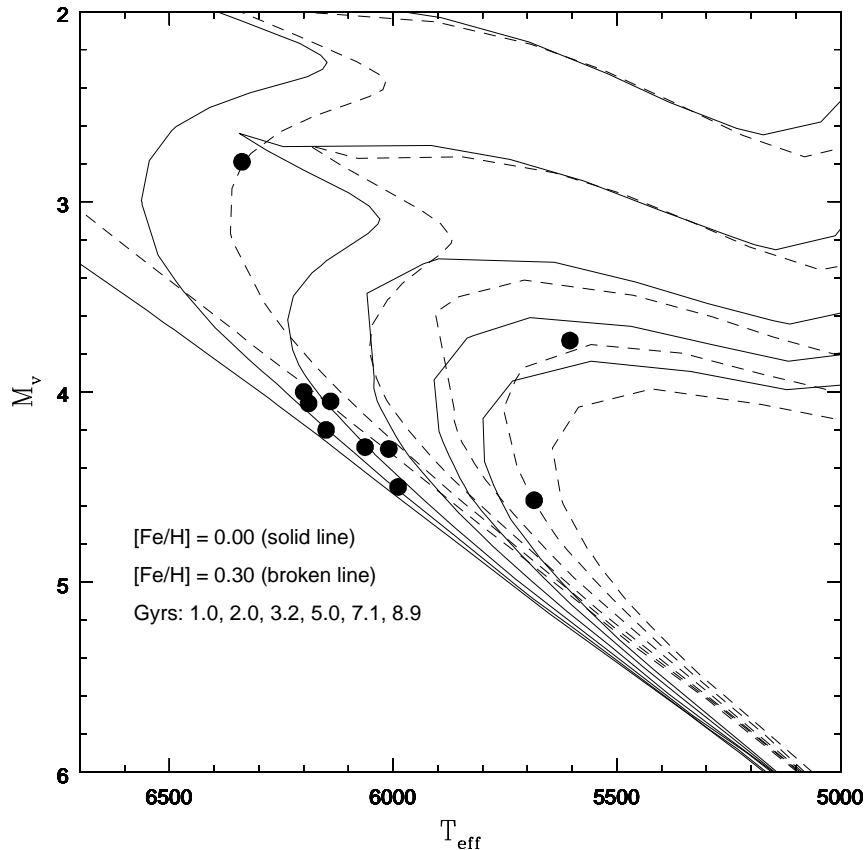


Figure 11. Age estimation using the isochrones computed by Girardi et al (2000) for program stars with planets.

cretion process and its benign effects on the structure of the star, the calculations show that accreted ${}^6\text{Li}$ (and ${}^7\text{Li}$) is preserved for more than 3 Gyr in stars of mass greater than about $1.1 M_{\odot}$. This limit corresponds to the effective temperature range $T_{\text{eff}} \geq 5900$ K. Lithium-7 is predicted to be completely preserved, a prediction at odds with the lithium abundances for field and cluster stars (Figure 12). This discrepancy could be removed by using alternative models, see, for example, the predictions given by Proffitt & Michaud (1989). One can infer from observations summarized in Figure 12 that accreted ${}^6\text{Li}$ will be depleted more quickly than predicted by Montalbán & Rebolo’s standard calculations: ${}^6\text{Li}$ seems likely to survive for only about 1 Gyr in main sequence stars with $T_{\text{eff}} \geq 6100$ K. (For $T_{\text{eff}} \sim 6600$ K, lithium is depleted to form the Boesgaard-dip [Boesgaard & Tripicco 1986]), but both isotopes may be quite similarly depleted.)

In the light of Figure 12 and Montalbán & Rebolo’s calculations, our failure to detect ${}^6\text{Li}$ in the young planet-hosting main sequence stars does not admit of a simple decisive conclusion about accretion of planets. Our measurements allow the following possibilities: (i) accretion has not occurred; (ii) accretion occurred but the accreted mass was insufficient to raise the star’s ${}^6\text{Li}$ abundance above our detection limit; and (iii) accretion occurred such that the post-accretion ${}^6\text{Li}$ abundance exceeded the detection limit but subsequent destruction of lithium depressed the ${}^6\text{Li}$ abundance again below the detection limit. Montalbán & Re-

bolo’s predictions of the survivability of ${}^6\text{Li}$ in stars with $M \geq 1.1 M_{\odot}$ and our failure to see ${}^6\text{Li}$ may suggest that accretion can rarely add more than a Jovian mass of ‘primordial’ material to the star. (Accretion of terrestrial rather than Jovian planets can effect an increase in the lithium abundances, but with a much smaller total mass for the accreted planets.)

Effects of accretion of planets on surface compositions are not limited to the lithium abundance. Accretion of circumstellar material has been invoked to account for the metallicity of planet-harboring stars. There is now a general consensus that such stars are more metal-rich than similar stars without planets (Gonzalez et al. 2001; Santos et al. 2001; Reid 2002), but the origin of this difference is still a matter of debate. Gonzalez (1997) suggested two possible explanations for the metallicity difference: accretion of H-poor matter (e.g., terrestrial planets, asteroids), and/or a bias in the discovery of planets in radial velocity surveys arising from a metallicity-dependent migration of giant planets toward the star. Gonzalez (1998) added a third possibility: a high metallicity of the natal cloud as a prerequisite for formation of giant planets. Santos et al. (2001) favoured this latter possibility. Combinations of these possibilities may need to be considered; for example, if high metallicity clouds are favoured sites for stars with planets, such stars may accrete planets, and if these planets are terrestrial in nature, the metallicity of the star will be further increased.

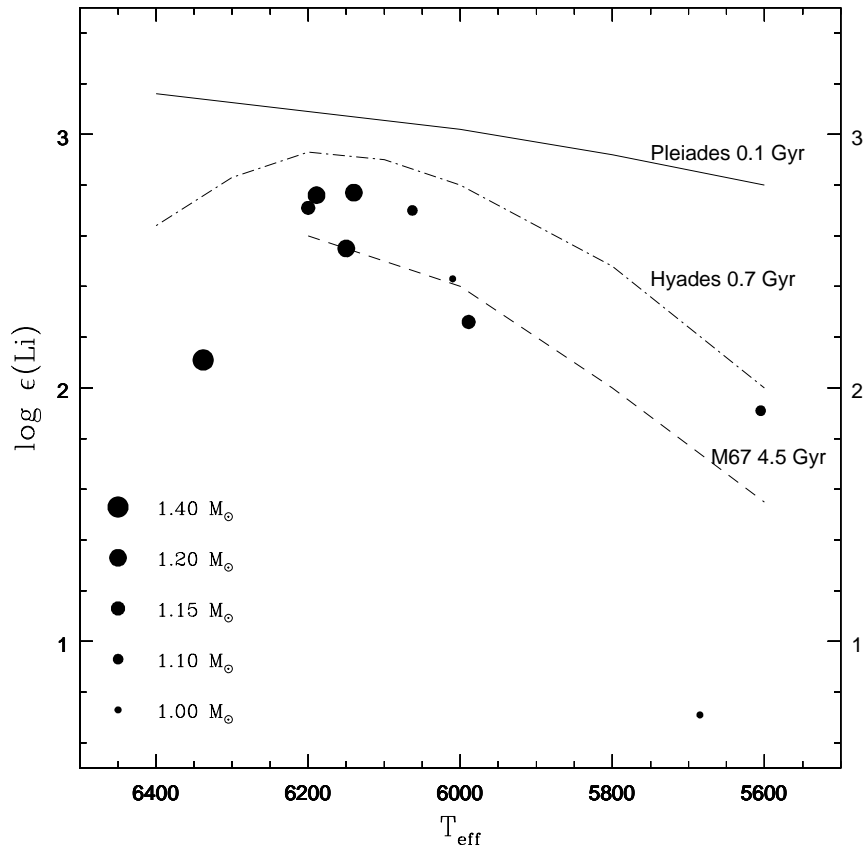


Figure 12. The derived Li abundances for planet hosting stars are compared with the Li abundances of Pleiades, Hyades and M67 clusters. Ages of the clusters are noted. The stellar masses of planet hosting stars are indicated by the size of the filled circles.

Observational evidence in support of accretion as the origin of the high metallicity of planet-hosting stars is limited. Detection of ${}^6\text{Li}$ in HD 82943 was claimed as supporting evidence. Our failure to confirm the presence of ${}^6\text{Li}$ weakens this claim, but, as we noted, accretion remains a possibility as long as ${}^6\text{Li}$ can be efficiently destroyed after the cessation of accretion. Accretion of giant planets will probably not change the surface composition of a star very much; giant planets are expected to have a composition similar to that of their host star, except for lithium and, perhaps, beryllium and boron. Since the composition of a terrestrial planet is far from a replica of the circumstellar material, the stellar composition will be changed by accretion of terrestrial planets. One expects volatile elements (e.g., C, N, and O) to be reduced, and the abundance of non-volatiles (e.g., Fe-peak elements) to be increased by accretion. A signature of accretion of terrestrial planets could be an abundance change correlated with an element's condensation temperature (T_c), the temperature at which an element condenses into solids as circumstellar gas cools in thermodynamic equilibrium. Gonzalez (1997) proposed this signature and searched for it in abundance analyses of two planet-hosting stars. Smith, Cunha, & Lazzaro (2001) noted that single (planet-less) metal-rich stars have a composition such that abundance differences, $[X/H]$ (relative to solar values) for element (X) are quite well correlated with T_c . These differences are,

therefore, plausibly attributed to Galactic chemical evolution, that is the net effect of nucleosynthesis by stars on the chemical composition of the interstellar medium. Stars hosting planets show the same abundance – T_c correlation at a given $[\text{Fe}/\text{H}]$ indicating that accretion of terrestrial planets can have more than a minor role in setting the stars' surface composition (see Takeda et al. 2001). Smith et al. did draw attention to a sample of five planet-hosting metal-rich stars for which the $[X/H]$ versus T_c correlation appeared unusually strong and suggested that accretion of terrestrial planets might have occurred in these cases. Four of the five stars are in Table 1.

Another example of a star which may have accreted dust, rocks, or terrestrial-like planets is HD 219542 A, a main sequence star with a distant main sequence companion. Gratton et al.'s (2001) differential abundance analysis found HD 219542 A overabundant relative to HD 219542 B in non-volatile elements but not in the volatile elements. The former were overabundant by about 0.07 dex. Gratton et al. remark that accretion of a few earth masses of rocky material by HD 219542 A would suffice to account for the differential abundances, and might also explain the different lithium abundances in primary and secondary; lithium's condensation temperature is similar to that of silicon and iron. HD 219542 A is one of our programme stars and the Li abundance (Table 2) agrees well with that given by Gratton

et al. (HD 219542 B is Li-poor, $\log \epsilon(\text{Li}) < 1.0$, according to Gratton et al.) The lithium abundance of HD 219542 A is 'normal' for this young star.

If accretion occurred and added lithium, the ${}^6\text{Li}$ abundance corresponding to a 0.07 dex increase in the iron abundance would be approximately $\log \epsilon({}^6\text{Li}) = -0.1$, if the accreted material contained a 'cosmic' abundance of lithium relative to iron. The corresponding ${}^7\text{Li}$ abundance is about $\log \epsilon({}^7\text{Li}) = 0.9$ in the absence of lithium at the stellar surface prior to accretion. The observed abundance is considerably higher implying, as expected from Figure 12, that substantial amounts of ${}^7\text{Li}$ were present when accretion occurred. Combining the observed ${}^7\text{Li}$ abundance with the inferred ${}^6\text{Li}$ abundance from the mass of accreted rocky material gives ${}^6\text{Li}/{}^7\text{Li} = 0.04$. We measure ${}^6\text{Li}/{}^7\text{Li} = 0.03 \pm 0.04$ which is consistent with the inference but also with an absence of ${}^6\text{Li}$. Inspection of the observed profile gives a tantalising impression of a break in the red wing due to ${}^6\text{Li}$ (Figure 7). Higher S/N spectra will be sought.

6 CONCLUDING REMARKS

Our search for ${}^6\text{Li}$ in the atmosphere of planet-hosting star proved unsuccessful, despite the intriguing earlier report of substantial amounts of ${}^6\text{Li}$ in HD 82943, a star known to host two giant planets. A limit of approximately ${}^6\text{Li}/{}^7\text{Li} \leq 0.03$ was set for eight planet-hosting stars including HD 82943. Detection of ${}^6\text{Li}$ in a late F/early G-dwarf was recognized by Israelian et al. (2001) as a possible signature of accretion of planets by a star. Non-detection of ${}^6\text{Li}$ is less than watertight evidence against such accretion. Searches for planets should in the near future identify much larger numbers of planet-hosting stars. Accretion of circumstellar material may also occur onto stars without a planetary system. A continued search for ${}^6\text{Li}$ may yield a positive detection of ${}^6\text{Li}$.

ACKNOWLEDGMENTS

We thank Carlos Allende Prieto, Gajendra Pandey, and Nils Ryde, for many spirited discussions, and UW group thanks Verne Smith for offering software. We thank Anita Cochran, Bill Cochran, Garek Israelian and Rafael Rebolo for their comments. The research of the UT group has been supported in part by National Science Foundation (grant AST 96-18414) and the Robert A. Welch Foundation of Houston, Texas. The UW group's research has been supported by a NASA Astrobiology Institute grant. This research has made use of the SIMBAD data base, operated at CDS, Strasbourg, France, and the NASA ADS service, USA.

REFERENCES

Allende Prieto, C., Asplund, M., García López, R.J., & Lambert, D.L. 2002, *ApJ*, 567, 544
 Allende Prieto, C & García López, R.J. 1998, *A&AS*, 129, 41
 Chen, Y.Q., Nissen, P.E., Zhao, G., Zhang, H.W., and Benoni, T. 2000, *A&AS*, 141, 491
 Balachandran, S. 1990, *ApJ*, 354, 310
 Bevington, R.P., & Robinson, D.K. 1992, in "Data Reduction and Error Analysis for the Physical Sciences", 2nd Edition (WCB McGraw-Hill)

Boesgaard, A.M., & Tripicco, M.J. 1986, *ApJ*, 303, 724
 Brault, J.W., & Müller, E.A. 1975, *Solar Physics*, 41, 43
 Brown, J.A., Sneden, C., Lambert, D.L., Dutchover, E. Jr. 1989, *ApJS*, 71, 293
 Fuhrmann, K. 1998, *A&A*, 338, 161
 Girardi, L., Bressan, A., Bertelli, G., & Chiosi, C. 2000, *A&A*, 371
 Giridhar, S., & Ferro, A.A. 1995, *Rev. Mex. Astron.Astrofis.*, 31, 23
 Gonzalez, G. 1997, *MNRAS*, 285, 403
 Gonzalez, G. 1998, *A&A*, 334, 221
 Gonzalez, G., Laws, C., Tyagi, S., Reddy, B. E. 2001, *AJ*, 121, 432
 Gratton, R.G., Bonanno, G., Claudi, R.U., Cosentino, R., Desidera, S., Lucatello, S., Scuderi, S. 2001, *A&A*, 377, 123
 Gray, D. F. 1992, *The Observation and Analysis of Stellar Photospheres* (Cambridge: Cambridge University Press)
 Gustafsson, B., Bell, R.A., Eriksson, K., Nordlund, Å. 1975, *A&A*, 42, 407
 Hinkle, K., Wallace, L., Valenti, J., & Harmer, D. 2000 *Visible and Near Infrared Atlas of the Arcturus Spectrum 3727 - 9300 Å* (San Francisco: ASP)
 Hobbs, L.M., Thorburn, J.A., & Rebull, L.M. 1999, *ApJ*, 523, 797
 Israelian, G., Santos, N.C., Mayor, M., & Rebolo, R. 2001, *Nature*, 411, 163
 Jones, B.F., Fischer, D., & Soderblom, D.R. 1999, *AJ*, 117, 330
 King, J.R., Deliyannis, C.P., Hiltgen, D.D., Stephens, A., Cunha, K., & Boesgaard, A.M. 1997, *AJ*, 113, 1871
 Kurucz, R., Furenlid, I., and Brault, J. 1984, *Solar Flux Atlas from 296 to 1300 nm* (New Mexico: National Solar Observatory)
 Kurucz, R. 1995: <http://cfaku5.harvard.edu>
 Lambert, D.L., Smith, V.V., & Heath, J. 1993, *PASP*, 105, 568
 Laws, C., & Gonzalez, G. 2001, *ApJ*, 553, 405
 Montalbán, J., & Rebolo, R. 2002, *A&A*, 386, 1039
 Nave, G., Johansson, S., Learner, R.C.M., Thorne, A.P., & Brault, J.W. 1994, *ApJS*, 94, 221
 Nissen, P.E., Lambert, D.L., Primas, F., & Smith, V.V. 1999, *A&A*, 348, 211
 Proffitt, C.R., & Michaud, G. 1989, *ApJ*, 345, 998
 Reid, I.N. 2002, *PASP*, 114, 306
 Santos, N.C., Israelian, G., and Mayor, M. 2000, *A&A*, 363, 228
 Santos, N.C., Israelian, G., and Mayor, M. 2001, *A&A*, 373, 1019
 Santos, N.C., García López, R.J., Israelian, G., Mayor, M., Rebolo, R., García-Gil, Pérez de Taoro, M.R., & Randich, S. 2002, *A&A*, 386, 1028
 Smith, V.V., Lambert, D.L., & Nissen P.E. 1998, *ApJ*, 506, 405
 Smith, V.V., Cunha, K., & Lazzaro, D. 2001, *AJ*, 121, 3207
 Sneden, C. 1973, Ph.D. thesis, Univ. Texas-Austin
 Takeda, Y. 1995, *PASJ*, 47, 337
 Takeda, Y. et al. 2001, *PASJ*, 53, 1211
 Tull, R.G., MacQueen, P.J., Sneden, C., & Lambert, D.L. 1995, *PASP*, 107, 251